Chemical Science

ROYAL SOCIETY OF CHEMISTRY

EDGE ARTICLE

View Article Online
View Journal | View Issue

Cite this: *Chem. Sci.*, 2022, **13**, 7310

All publication charges for this article have been paid for by the Royal Society of Chemistry

Received 15th December 2021
Accepted 31st May 2022

DOI: 10.1039/d1sc06986a

rsc.li/chemical-science

Rh(I)-catalyzed dimerization of ene-vinylidenecyclopropanes for the construction of spiro[4,5]decanes and mechanistic studies†

Chao Ning,[a] Kang-Hua Rui,[a] Yin Wei *[b] and Min Shi *[ab]

Rh(I) complex catalyzed dimerization of ene-vinylidenecyclopropanes took place smoothly to construct a series of products containing spiro[4,5]decane skeletons featuring a simple operation procedure, mild reaction conditions, and good functional group tolerance. In this paper, the combination of experimental and computational studies reveals a counterion-assisted Rh(I)–Rh(III)–Rh(V)–Rh(III)–Rh(I) catalytic cycle involving tandem oxidative cyclometallation/reductive elimination/selective oxidative addition/selective reductive elimination/reductive elimination steps; in addition, a pentavalent spiro-rhodium intermediate is identified as the key intermediate in this dimerization reaction upon DFT calculation.

Introduction

Spiro[4,5]decanes and polycyclic natural products containing the spiro[4,5]decane moiety possessing useful biological properties are important resources in medicinal chemistry and the pharmaceutical industry.[1,2] One of the representative bioactive molecules containing the spiro[4,5]decane moiety is β-vetivone (Fig. 1), which was first isolated from *Vetiveria zizanioides* in 1939 by Pfau and Plattner.[2a] Since then, more and more natural products containing the spiro[4,5]decane skeleton with biological activity have been isolated and synthesized by organic chemists.[2d] Several representative compounds are shown in Fig. 1. For example, hinesol may represent a novel medicinal drug having indications in the treatment of leukemia. Sequosempervirin A isolated from *Sequoia sempervirens* is also expected to exhibit useful biological activity.[2f] In addition, the guaianolide-type sesquiterpenoid dimers are known as a unique array of sesquiterpenoid natural products and show biological antitumor and anti-HIV activity. In view of their excellent biological activity, it is of significant interest to introduce the spiro[4,5]decane skeleton into pharmaceutically active molecules for further research.

It has always been challenging to construct the spiro quaternary carbon stereocenter, because the formation of the spiro quaternary carbon stereocenter needs to overcome strong steric hindrance and ring strain.[3] Therefore, in the past few decades, significant efforts have been devoted to the development of novel strategies to build all-carbon spirocyclic ring systems.[4] The transition metal-catalyzed domino cyclization of 1,*n*-enynes and 1,*n*-dienes serves as a useful strategy for the synthesis of cyclic products.[5] In the metal-catalyzed domino cyclization reaction, the formation of multiple C–C bonds can be controlled by choosing different metals (*e.g.*, Rh,[6] Co,[7] Ni,[8] *etc.*[9]) and ligands to control the chemo-, regio- and stereoselectivity, involving interesting mechanisms. In the metal-catalyzed domino cyclization process, the cyclometallation of the [1,*n*]-π-system provides the key intermediate, which subsequently undergoes migration and insertion of the unsaturated bonds of alkenes, alkynes, or allenes *via* an intramolecular or intermolecular mode (Scheme 1). In most cases, the products

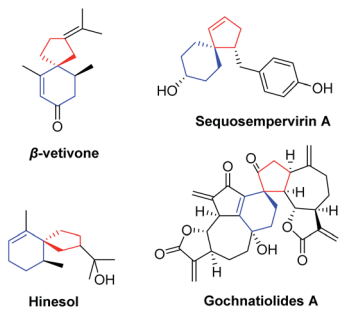

Fig. 1 Representative bioactive compounds containing the spiro[4,5] decane moiety.

[a]*Key Laboratory for Advanced Materials and Institute of Fine Chemicals, Key Laboratory for Advanced Materials, Feringa Nobel Prize Scientist Joint Research Center, School of Chemistry & Molecular Engineering, East China University of Science and Technology, Meilong Road No. 130, Shanghai, 200237, China. E-mail: mshi@mail.sioc.ac.cn*

[b]*State Key Laboratory of Organometallic Chemistry, Center for Excellence in Molecular Synthesis, University of Chinese Academy of Sciences, Shanghai Institute of Organic Chemistry, Chinese Academy of Sciences, 345 Lingling Road, Shanghai 200032, China. E-mail: weiyin@sioc.ac.cn*

† Electronic supplementary information (ESI) available: Experimental procedures and characterization data of new compounds. CCDC 1563064. For ESI and crystallographic data in CIF or other electronic format see https://doi.org/10.1039/d1sc06986a

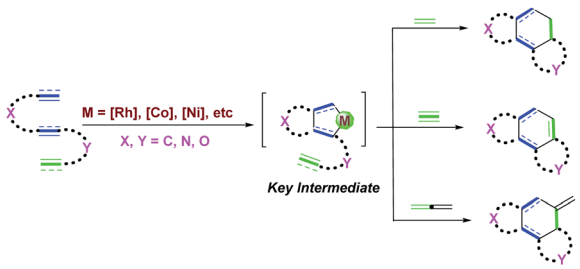

Scheme 1 General model of the transition metal-catalyzed domino cyclization of 1,*n*-enynes and 1,*n*-dienes.

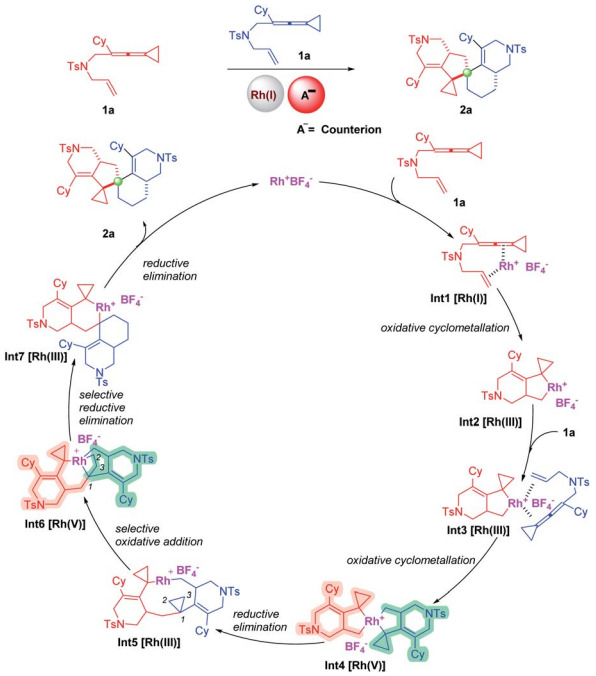

Scheme 2 This work and proposed mechanism.

containing fused rings are usually accessed through metal-catalyzed domino cyclization reactions. There are only a few reports on the construction of spirocyclic compounds through rational design of substrates and novel mechanisms.[10]

In this work, we report a dimerization reaction of ene-vinylidenecyclopropanes (ene-VDCPs) as an effective and facile method to provide a series of compounds containing spiro[4,5] decane skeletons (Scheme 2, this work). A plausible mechanism is proposed as outlined in Scheme 2. First, the coordination of Rh(I) with the allene moiety and olefin moiety in an ene-VDCP leads to the formation of intermediate **Int1**.

Subsequent cyclometallation then gives the rhodacyclic intermediate **Int2**.[11] The intermediate **Int2** is coordinated with another molecular ene-VDCP to produce intermediate **Int3**, which undergoes a cyclometallation to afford the spirocyclic rhodium(V) intermediate **Int4**.[12,13] Reductive elimination affords medium-membered rhodacyclic intermediate **Int5**. The rhodium(III) inserts into the C_1–C_2 bond or C_1–C_3 of the distal cyclopropane to generate the rhodium(V) intermediate **Int6**. Subsequently, the rhodium(V) intermediate **Int6** undergoes reductive elimination to afford intermediate **Int7**, which then produces product **2a** through reductive elimination and regenerates the catalyst. Herein, the exploration of the substrate scope of this novel domino dimerization process and the detailed mechanistic investigations will be performed to study the suggested reaction mechanism in this context.

Results and discussion

Experimental investigations

At the start of our studies, ene-VDCP **1a** was used as the model substrate to test the reaction outcome. Interestingly, the reaction successfully took place in the presence of 5 mol% $Rh(cod)_2BF_4$ in anhydrous toluene at 80 °C after 8 hours and the dimerization product **2a** was obtained in 40% isolated yield (Table 1, entry 1). Upon lowering the reaction temperature to 60 °C, the target product was obtained in 60% yield (entry 2). Gratifyingly, taking the combination of $[Rh(cod)Cl]_2$ and $AgBF_4$ could afford the desired product **2a** in 85% yield at 60 °C (entry 3). Accordingly, a series of additives were screened, such as Ag salts, Lewis acids and $NaBAr^F{}_4$, and none of them showed a better yield to obtain the desired product than the combination of $[Rh(cod)Cl]_2$ and $AgBF_4$ (entries 4–10). Screening different solvents implied that toluene was the most optimal solvent for this reaction (entry 3 *vs.* entries 11–15). Increasing the amount of additive to 20 mol% did not have a great effect on

Table 1 Optimization of the reaction conditions[a]

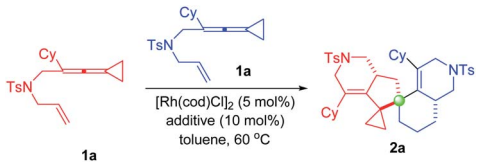

Entry	Catalyst	Additive	T (°C)	Solvent	Yield[b] (%)
1	$Rh(cod)_2BF_4$	—	80	Toluene	40
2	$Rh(cod)_2BF_4$	—	60	Toluene	60
3	**$[Rh(cod)Cl]_2$**	**$AgBF_4$**	**60**	**Toluene**	**85**
4	$[Rh(cod)Cl]_2$	AgOTf	60	Toluene	62
5	$[Rh(cod)Cl]_2$	$AgNTf_2$	60	Toluene	—
6	$[Rh(cod)Cl]_2$	$AgSbF_6$	60	Toluene	—
7	$[Rh(cod)Cl]_2$	$Sc(OTf)_3$	60	Toluene	34
8	$[Rh(cod)Cl]_2$	$Yb(OTf)_3$	60	Toluene	32
9	$[Rh(cod)Cl]_2$	$In(OTf)_3$	60	Toluene	28
10	$[Rh(cod)Cl]_2$	$NaBAr^F{}_4$	60	Toluene	—
11	$[Rh(cod)Cl]_2$	$AgBF_4$	60	PhCl	60
12	$[Rh(cod)Cl]_2$	$AgBF_4$	60	DCE	78
13	$[Rh(cod)Cl]_2$	$AgBF_4$	60	THF	70
14	$[Rh(cod)Cl]_2$	$AgBF_4$	60	Dioxane	72
15	$[Rh(cod)Cl]_2$	$AgBF_4$	60	MeCN	Trace
16[c]	$[Rh(cod)Cl]_2$	$AgBF_4$	60	Toluene	86

[a] Reaction conditions: **1a** (0.20 mmol), catalyst (5 mol%), additive (10 mol%), solvent (2 mL), 8 h, Ar. All the reactions were carried out on a 0.20 mmol scale in solvent (2 mL) at 60 °C for 8 h unless otherwise specified. [b] Isolated yield. [c] 20 mol% additive was added.

the yield (entry 16). Next, we tried to explore the asymmetric variants of this dimerization reaction by using chiral binaphthyl bisdiarylphosphine ligands. When the ligand was added, the yield of the desired product slightly decreased; the corresponding stereoselective product was not obtained, suggesting that the ligands did not play roles in this reaction, probably due to the key intermediate **Int2** preferring to coordinate with another substrate molecule (for more details, see Table S1 on page S5 in the ESI†).

With the optimized reaction conditions identified, the substrate scope for the dimerization of ene-VDCPs **1** was then explored and the results are shown in Table 2. The X-ray diffraction pattern of **2a** is shown in Table 2, whose structure had been unambiguously determined. The related CIF data of **2a** are shown in the ESI.† Firstly, changing the *N*-linked ene-VDCPs to *N*-*p*-bromobenzenesulfonyl (NBs) and NSO_2Ph yielded similar results, producing the dimerization products **2b** and **2c** in 75% yield and 72% yield, respectively. However, upon changing the linker as *N*-methylsulfonyl (NMs), the expected product **2d** was not detected. To our delight, upon changing the linker as an oxygen atom, the desired product **2e** was obtained in 48% yield. Unfortunately, no desired reaction occurred using the CH_2-linked substrate **1f** presumably due to the skeleton structure of the full carbon chain not being conducive to the generation of cyclometalated species. Next, the R moiety of substrates **1** was investigated. For substrates containing alkyl substituents including cycloalkane substituents, the reactions took place smoothly, giving the target products **2g–2j** in 78–82% yields. However, employing substrates **1k** and **1l** with a cyclopropyl and a cyclobutyl group as a substituent, the desired products **2k** and **2l** were not obtained under the standard conditions. Then, various substituents on the benzene ring were tested. Neither electron-rich nor electron-poor aromatic rings have an obvious impact on the reaction activity, and the desired products **2m–2w** were obtained in good yields ranging from 60% to 85%. Substrate **1x** with an *ortho*-substituted methyl group did not proceed under the standard reaction conditions, probably due to the steric hindrance of the *ortho*-substituent. As for substrate **1y**, the reaction proceeded smoothly to give the desired product **2y** in 76% yield. Product **2z**, bearing a benzo[*d*][1,3]dioxole moiety, could also be obtained in 60% yield. We further conducted an investigation on other aromatic rings such as naphthalene or thiophene substituted substrates and obtained the corresponding products **2aa** and **2ab** in 78% yield

Table 2 Substrate scope of ene-vinylidenecyclopropanes **1**[a]

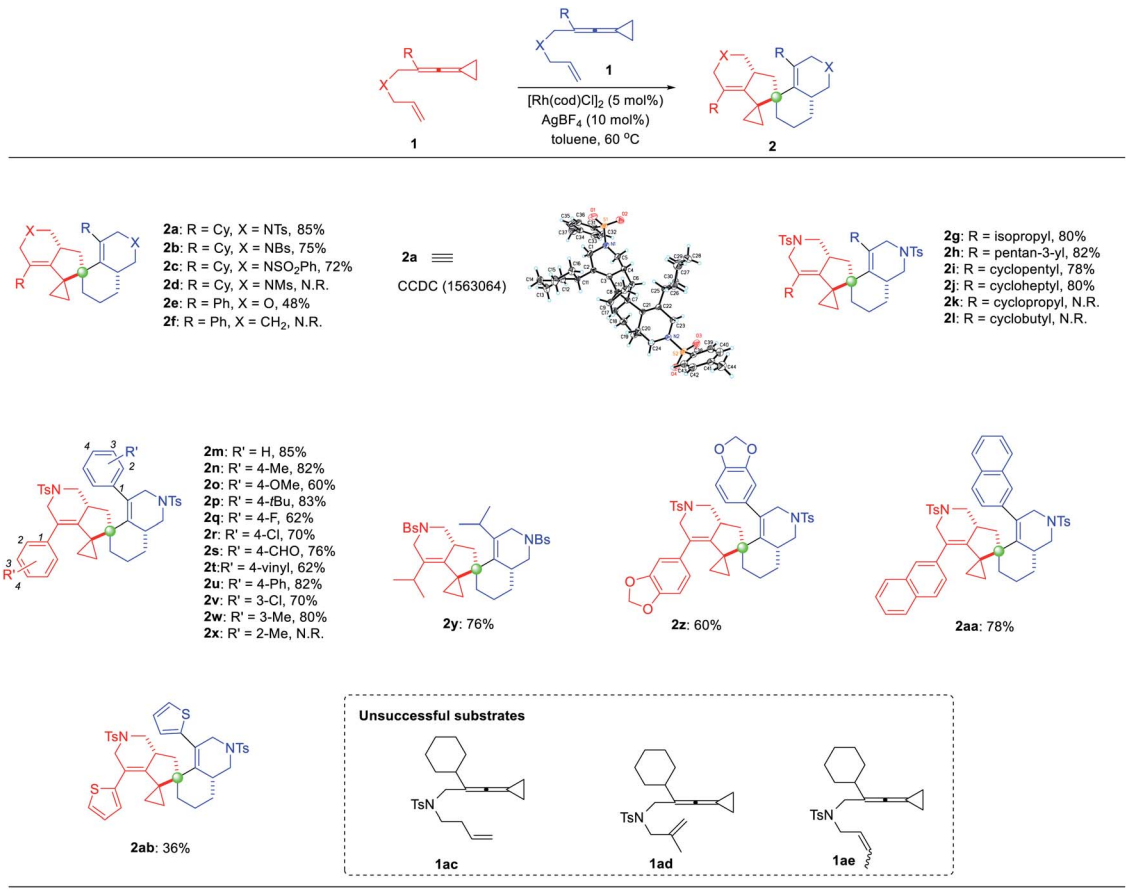

[a] Reaction conditions: **1** (0.20 mmol), catalyst (5 mol%), additive (10 mol%), solvent (2 mL), 60 °C, 8 h, Ar. Yields were determined from isolated products.

and 36% yield, respectively. Upon extending the carbon linker as for substrate **1ac** or introducing a substituent at the olefin moiety as for substrates **1ad** and **1ae**, none of the desired spirocyclic dimers were formed, presumably due to the steric issue.

In order to investigate the regio- and chemoselectivity of the dimerization of ene-vinylidenecyclopropanes, we attempted the cross-over experiments. Under the standard conditions, we performed cross-over experiments on substrates **1a** and **1m**. We obtained a mixture of products **2a**, **2m** and cross-over products **2am** and **2ma** (Scheme 3a). The products **2a**, **2m** and cross-over products **2am** and **2ma** were identified by high-resolution mass spectrometry [HRMS (ESI) *m*/*z*: $(M + H)^+$ calcd for $C_{44}H_{53}N_2O_4S_2$: 737.3447, found: 737.3448] (Scheme 3a). Based on the new signals of cyclopropanes in the ^{1}H NMR spectra of the mixture, the cross-over products were also confirmed (for more details, see page S7 in the ESI†). Unfortunately, because the polarities of these compounds are too close, it is difficult for us to separate these compounds. We further used substrates **1c** without the Ts functional group and **1p** to conduct the cross-over experiment. Similarly, we obtained a mixture of products **2c**, **2p** and cross-over products **2cp** and **2pc** (Scheme 3b). The products **2c**, **2p** and cross-over products **2cp** and **2pc** were also identified by high-resolution mass spectrometry [HRMS (ESI) *m*/*z*: $(M + H)^+$ calcd for $C_{47}H_{59}N_2O_4S_2$: 779.3916, found: 779.3914] (Scheme 3b). Based on the ^{1}H NMR spectra of the mixture, we found the signals of a new T_s group and *tert*-butyl group, which confirmed the formation of cross-over products (see page S9 in the ESI†). However, the products were not isolated due to the close polarities of these compounds.

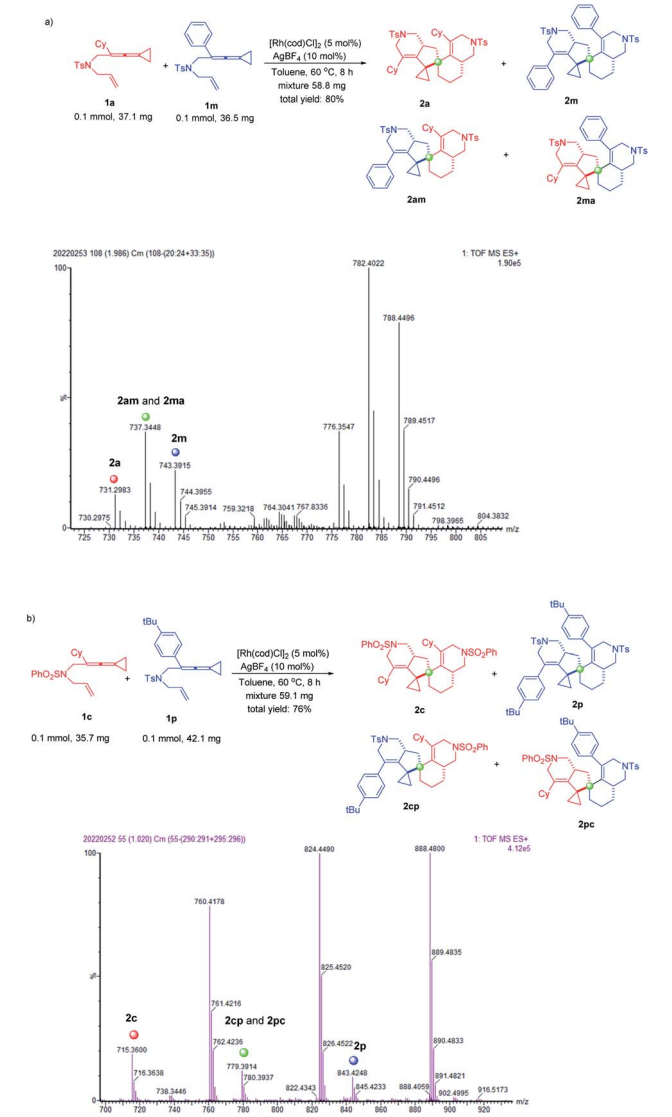

Scheme 3 Cross-over experiments of (a) **1a** and **1m**, and (b) **1c** and **1p**.

Synthetic applications

In order to explore the synthetic applicability of this protocol, scale-up (half-gram) reactions were carried out. As shown in Scheme 4, these reactions were conducted employing 2.00 mmol of **1a** or **1m**, producing 0.563 g of **2a** and 0.584 g of **2m** in 76% yield and 80% yield under the standard conditions, respectively (Scheme 4a). Furthermore, we demonstrated the synthetic utility of the spiro[4,5]decane products, showing that the *N*-tosyl group of **2m** was removed upon treating with sodium naphthalenide in THF at −78 °C, affording product **3** in only 36% yield, probably due to its instability (Scheme 4b). Several further synthetic transformations were attempted; however, we did not obtain the desired products (for details, see the ESI from page S11 to page S13†).

Mechanistic studies

To further understand the mechanism, we carried out a series of control experiments and density functional theory (DFT) calculations. We first proposed a possible mechanism involving rhodium carbenoid and silver carbenoid intermediates as key intermediates (see Scheme S1 in the ESI†). However, the suggested key silver carbene intermediate is not stable and cannot be located by DFT calculations (for details, see the ESI†), so we excluded this mechanism. Then, we proposed another mechanism involving a rhodium carbenoid intermediate accompanied by a [2 + 2 + 1] cycloaddition reaction with another

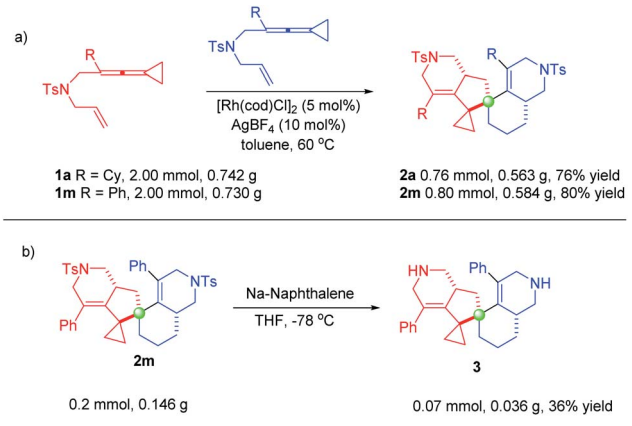

Scheme 4 (a) Scale-up (half-gram) experiments; (b) synthetic transformations.

molecular substrate[14] (for more details, see Scheme S1 in the ESI†) and a mechanism involving the spiro rhodium(v) intermediate shown in Scheme 2. We attempted to capture the possible rhodium carbenoid intermediates by trapping experiments with styrene or pyridine *N*-oxides; however, we did not succeed in these trapping experiments (Scheme 5a). We subsequently embarked on DFT calculations to gain insight into the reaction mechanism. All calculations have been

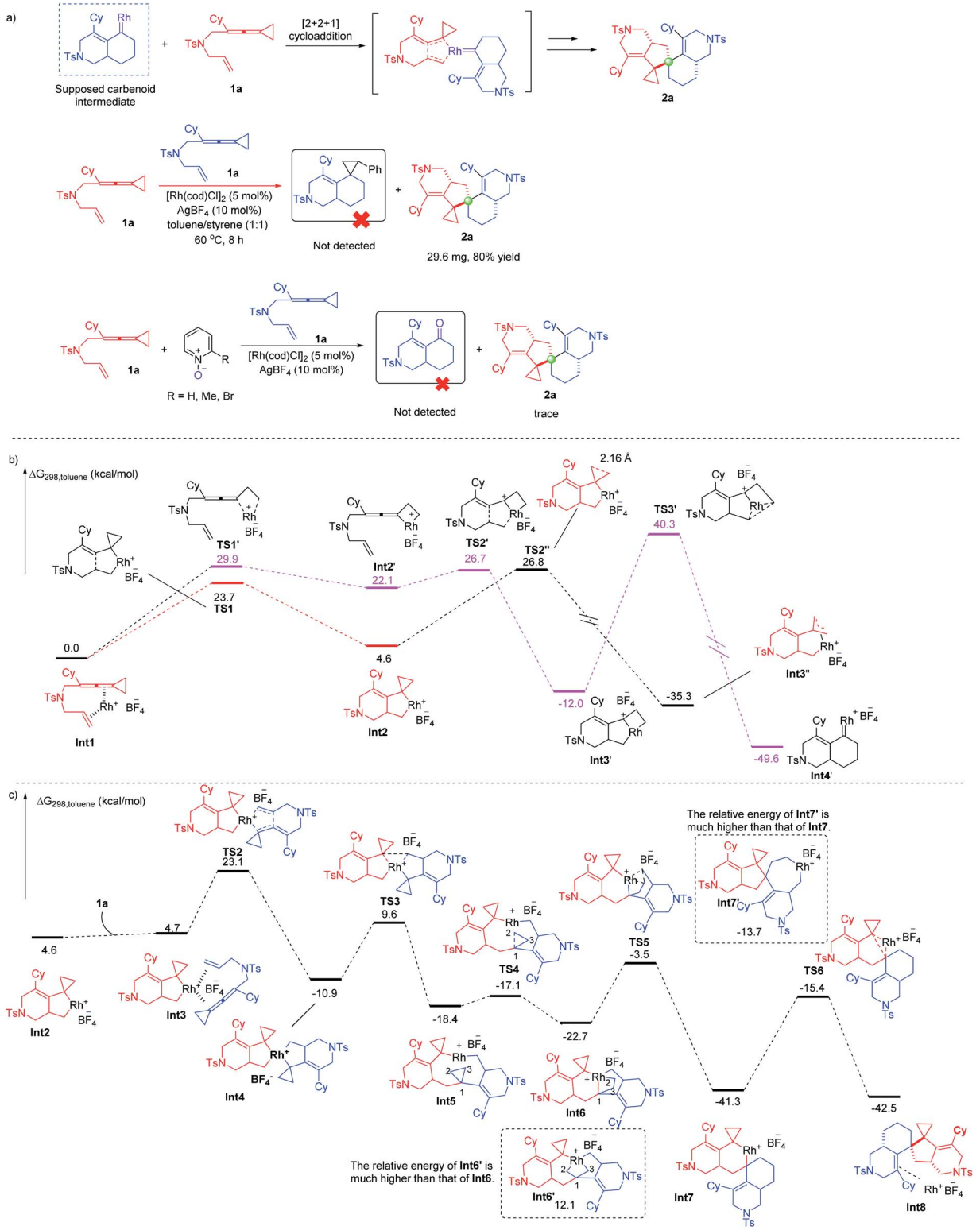

Scheme 5 (a) Control experiments; (b) DFT calculations on the possible pathways for generation of key intermediates; (c) DFT calculations on the possible pathways for formation of product **2a**.

performed at the SMD/B3LYP/6-311+G(d,p)/Lanl2dz//B3LYP/6-31G(d)/Lanl2dz level with the Gaussian 16 program. We investigated the reaction pathway starting from a stable rhodium complex **Int1** (shown in Scheme 5b), in which both the alkene and the allene units of **1a** are coordinated to the rhodium catalyst. **Int1** can undergo an oxidative cyclometallation to give a rhodacyclic intermediate **Int2** through **TS1** with an energy barrier of 23.7 kcal mol^{-1}. It should be mentioned here that without the assistance of a counterion (BF_4^-) the intermediate **Int2** is unstable; this result may account for why an amount of additive ($AgBF_4$) is necessary in experiments. Alternatively, **Int1** can be transformed into intermediate **Int2′** *via* **TS1′**, with an energy barrier of 29.9 kcal mol^{-1} in a highly endothermic process (ΔG = 22.1 kcal mol^{-1}). The intermediate **Int2′** subsequently undergoes cyclometallation to generate an intermediate **Int3′** *via* transition state **TS2′**. Passing through transition state **TS3′** with an extremely high energy barrier of 52.3 kcal mol^{-1}, the intermediate **Int3′** can transform into a very stable rhodium carbene intermediate **Int4′**. Although the rhodium carbene intermediate **Int4′** is thermodynamically stable, an extremely high energy barrier needs to be overcome, which cannot be achieved under our experimental conditions. Thus, the suggested mechanism involving the rhodium carbene intermediate (see page S15 in the ESI†) is excluded. We also investigated whether the intermediate **Int2** can undergo a β-C elimination. This step is not a canonical β-C elimination, but instead consists of a distal opening of the cyclopropyl ring (C···C bond distance of 2.16 Å in **TS2″**), a process reminiscent to that previously proposed for cyclopropyl Rh(III) complexes and other transition metal derivatives. Passing through transition state **TS2″** with an energy barrier of 22.2 kcal mol^{-1}, a TMM metal complex **Int3″** is generated.

Next, we continued to investigate the following reaction steps through computational studies (Scheme 5c). The rhodacyclic intermediate **Int2** can associate with another molecule of substrate **1a** to generate a rhodium complex **Int3** since there is no ligand in the presence of the reaction system. Interestingly, **Int3** can undergo another cyclometallation to generate an uncommonly stable spiro rhodium(V) intermediate **Int4** *via* transition state **TS2** in an exothermic process (ΔG = −15.6 kcal mol^{-1}). The energy barrier for cyclometallation is 18.4 kcal mol^{-1}, which is lower than that of the competitive pathway involving the so-called β-C elimination step (22.2 kcal mol^{-1} *via* **TS2″**). Thus, we exclude the β-C elimination pathway, which is similar to the Co-catalyzed cycloaddition reaction of ACPs.[7b] The subsequent reductive elimination step takes place through transition state **TS3** with an energy barrier of 20.5 kcal mol^{-1} to afford intermediate **Int5** having a nine-membered ring. Similarly, the competitive pathway involving the so-called β-C elimination of **Int4** is ruled out due to the higher energy barrier (for details, see Scheme S4 on page S123 in the ESI†). Instead of insertion into the neighboring cyclopropane, the rhodium(III) prefers to insert into the C–C bond of the distal cyclopropane to generate another rhodium(V) intermediate **Int6** *via* **TS4** with a small energy barrier (1.3 kcal mol^{-1}), probably due to the flexibility of the geometry of the medium-sized ring.[15] An alternative intermediate **Int6′** was also investigated; however, its energy is much higher than that of **Int6** by 34.8 kcal mol^{-1}. Subsequently, the rhodium(V) intermediate **Int6** undergoes a reductive elimination step to produce intermediate **Int7** *via* transition state **TS5**; another possible intermediate **Int7′** is also investigated. However, intermediate **Int7′** is discarded since its energy is much higher than that of **Int7** by 27.6 kcal mol^{-1}. Finally, intermediate **Int7** undergoes another reductive elimination step to produce the product complex **Int8** through transition state **TS6** with an energy barrier of 25.9 kcal mol^{-1}, which is the highest barrier in the whole reaction pathway. The calculation results provide theoretical evidence for the proposed mechanism shown in Scheme 2. We also investigated another possible reaction pathway where **int2** inserts into the allene moiety of another **1a**, and β-C elimination takes place to open the cyclopropane ring; then the resulting intermediate inserts back into the allene and then the alkene, followed by reductive elimination to afford the product (for details, see Schemes S2 and S3 on pages S16 and S17 in the ESI†). However, the whole process involving Rh(I)–Rh(III)–Rh(I) involves intermediates and transition states that have the higher energies than the key intermediates and transition states in the redox-neutral Rh(I)–Rh(III)–Rh(V)–Rh(III)–Rh(I) catalytic cycle. Thus, a redox-neutral Rh(I)–Rh(III)–Rh(V)–Rh(III)–Rh(I) catalytic cycle assisted by a counterion, involving tandem oxidative cyclometallation/reductive elimination/selective oxidative addition/selective reductive elimination/reductive elimination steps for this dimerization reaction, was deduced based on a series of mechanistic investigations.

Conclusions

In conclusion, we have developed an efficient protocol for the Rh(I)-catalyzed dimerization reaction of ene-vinylidenecyclopropanes, delivering products containing spiro [4,5]decane skeletons in moderate to good yields with a wide substrate scope and good functional group tolerance. In addition, this reaction was achieved on a half-gram scale, and the corresponding products could be further transformed into synthetically interesting compounds. Systematic mechanistic studies, supported by DFT calculations, allowed us to propose a plausible counterion-assisted Rh(I)–Rh(III)–Rh(V)–Rh(III)–Rh(I) reaction mechanism. Further investigations with regard to the construction of related spirocyclic compounds, which may have useful applications in the synthesis of drug-like substances, and other functional materials under Rh(I) catalysis are underway in our laboratory.

Data availability

Experimental and computational data have been made available as ESI.†

Author contributions

C. N. and K.-H. R. contributed to the experimental work. Y. W. contributed to the computational work. C. N., Y. W. and M. S. contributed to ideation and writing of the paper.

Conflicts of interest

There are no conflicts to declare.

Acknowledgements

We are thankful for the financial support from the National Natural Science Foundation of China (21121062, 21302203, 21372250, 21772037, 21772226, 21861132014, 91956115 and 22171078), the project supported by Shanghai Municipal Science and Technology Major Project (Grant No. 2018SHZDZX03) and the Fundamental Research Funds for the Central Universities (222201717003).

References

1 (*a*) M. Vandewalle and P. De Clercq, *Tetrahedron*, 1985, **41**, 1765–1831; (*b*) W. G. Dauben and D. J. Hart, *J. Am. Chem. Soc.*, 1977, **99**, 7307–7314; (*c*) A. R. Díaz-Marrero, G. Porras, Z. Aragón, J. M. de la Rosa, E. Dorta, M. Cueto, L. D'Croz, J. Maté and J. Darias, *J. Nat. Prod.*, 2011, **74**, 292–295; (*d*) S. Kováčová, S. K. Adla, L. Maier, M. Babiak, Y. Mizushina and K. Paruch, *Tetrahedron*, 2015, **71**, 7575–7582; (*e*) J.-R. Huang, M. Sohail, T. Taniguchi, K. Monde and F. Tanaka, *Angew. Chem., Int. Ed.*, 2017, **56**, 5853–5857.

2 (*a*) A. S. Pfau and P. A. Plattner, *Helv. Chim. Acta*, 1939, **22**, 640–654; (*b*) J. A. Marshall and P. C. Johnson, *J. Am. Chem. Soc.*, 1967, **89**, 2750–2751; (*c*) E. Wenkert, B. L. Buckwalter, A. A. Craveiro, E. L. Sanchez and S. S. Sathe, *J. Am. Chem. Soc.*, 1978, **100**, 1267–1273; (*d*) Y. Ito, K. Takahashi, H. Nagase and T. Honda, *Org. Lett.*, 2011, **13**, 4640–4643; (*e*) C. Li, L. Dian, W. Zhang and X. Lei, *J. Am. Chem. Soc.*, 2012, **134**, 12414–12417; (*f*) H. B. Park, Y.-J. Kim, J. K. Lee, K. R. Lee and H. C. Kwon, *Org. Lett.*, 2012, **14**, 5002–5005; (*g*) L. K. Smith and I. R. Baxendale, *Org. Biomol. Chem.*, 2015, **13**, 9907–9933; (*h*) P. Luo, Y. Cheng, Z. Yin, C. Li, J. Xu and Q. Gu, *J. Nat. Prod.*, 2019, **82**, 349–357.

3 (*a*) V. A. D'yakonov, O. A. Trapeznikova, A. de Meijere and U. M. Dzhemilev, *Chem. Rev.*, 2014, **114**, 5775–5814; (*b*) Y. Li and S. Xu, *Chem.–Eur. J.*, 2018, **24**, 16218–16245; (*c*) Z. Wang, Z.-P. Yang and G. C. Fu, *Nat. Chem.*, 2021, **13**, 236–242.

4 (*a*) R. Rios, *Chem. Soc. Rev.*, 2012, **41**, 1060–1074; (*b*) A. K. Franz, N. V. Hanhan and N. R. Ball-Jones, *ACS Catal.*, 2013, **3**, 540–553; (*c*) L. K. Smith and I. R. Baxendale, *Org. Biomol. Chem.*, 2015, **13**, 9907–9933; (*d*) M.-Y. Wu, W.-W. He, X.-Y. Liu and B. Tan, *Angew. Chem., Int. Ed.*, 2015, **54**, 9409–9413; (*e*) D.-Z. Chen, W.-J. Xiao and J.-R. Chen, *Org. Chem. Front.*, 2017, **4**, 1289–1293; (*f*) J.-H. Ye, L. Zhu, S.-S. Yan, M. Miao, X.-C. Zhang, W.-J. Zhou, J. Li, Y. Lan and D.-G. Yu, *ACS Catal.*, 2017, **7**, 8324–8330; (*g*) A. Ding, M. Meazza, H. Guo, J. W. Yang and R. Rios, *Chem. Soc. Rev.*, 2018, **47**, 5946–5996; (*h*) P. Bunse, C. Schlepphorst, F. Glorius, M. Kitamura and B. Wünsch, *J. Org. Chem.*, 2019, **84**, 13744–13754; (*i*) J. Ma, F. Schäfers, C. Daniliuc, K. Bergander, C. A. Strassert and F. Glorius, *Angew. Chem., Int. Ed.*, 2020, **59**, 9639–9645.

5 (*a*) Y. Yamamoto, *Chem. Rev.*, 2012, **112**, 4736–4769; (*b*) Y. Shibata and K. Tanaka, *Synthesis*, 2012, **44**, 323–350; (*c*) A. Lledó, A. Pla-Quintana and A. Roglans, *Chem. Soc. Rev.*, 2016, **45**, 2010–2023; (*d*) G. Domínguez and J. Pérez-Castells, *Chem.–Eur. J.*, 2016, **22**, 6720–6739; (*e*) A. Roglans, A. Pla-Quintana and M. Solà, *Chem. Rev.*, 2021, **121**, 1894–1979.

6 (*a*) T. Sato, *Nippon Kagaku Zassi*, 1971, **92**, 277–296; (*b*) Y. Wang and Z.-X. Yu, *Acc. Chem. Res.*, 2015, **48**, 2288–2296; (*c*) Y. Ohta, S. Yasuda, Y. Yokogawa, K. Kurokawa and C. Mukai, *Angew. Chem., Int. Ed.*, 2015, **54**, 1240–1244; (*d*) K. Masutomi, H. Sugiyama, H. Uekusa, Y. Shibata and K. Tanaka, *Angew. Chem., Int. Ed.*, 2016, **55**, 15373–15376; (*e*) H. Ueda, K. Masutomi, Y. Shibata and K. Tanaka, *Org. Lett.*, 2017, **19**, 2913–2916; (*f*) S. Yoshizaki, Y. Shibata and K. Tanaka, *Angew. Chem., Int. Ed.*, 2017, **56**, 3590–3593; (*g*) Z. Tian, Q. Cui, C. Liu and Z. Yu, *Angew. Chem., Int. Ed.*, 2018, **57**, 15544–15548; (*h*) L. Deng, Y. Fu, S. Y. Lee, C. Wang, P. Liu and G. Dong, *J. Am. Chem. Soc.*, 2019, **141**, 16260–16265; (*i*) S.-H. Hou, X. Yu, R. Zhang, L. Deng, M. Zhang, A. Y. Prichina and G. Dong, *J. Am. Chem. Soc.*, 2020, **142**, 13180–13189; (*j*) Y. Wang, W. Liao, Y. Wang, L. Jiao and Z.-X. Yu, *J. Am. Chem. Soc.*, 2022, **144**, 2624–2636.

7 (*a*) A. Geny, S. Gaudrel, F. Slowinski, M. Amatore, G. Chouraqui, M. Malacria, C. Aubert and V. Gandon, *Adv. Synth. Catal.*, 2009, **351**, 271–275; (*b*) E. Da Concepción, I. Fernández, J. L. Mascareñas and F. López, *Angew. Chem., Int. Ed.*, 2021, **60**, 8182–8188; (*c*) T. Yasui, R. Tatsumi and Y. Yamamoto, *ACS Catal.*, 2021, **11**, 9479–9484; (*d*) J. H. Herbort, R. F. Lalisse, C. M. Hadad and T. V. RajanBabu, *ACS Catal.*, 2021, **11**, 9605–9617; (*e*) X. Xiao and Z. Yu, *Chem.–Eur. J.*, 2021, **27**, 7176–7182.

8 (*a*) M. Shanmugasundaram, M.-S. Wu and C.-H. Cheng, *Org. Lett.*, 2001, **3**, 4233–4236; (*b*) T. Kawasaki, S. Saito and Y. Yamamoto, *J. Org. Chem.*, 2002, **67**, 4911–4915; (*c*) M. Shanmugasundaram, M.-S. Wu, M. Jeganmohan, C.-W. Huang and C.-H. Cheng, *J. Org. Chem.*, 2002, **67**, 7724–7729; (*d*) T. N. Tekavec and J. Louie, *J. Org. Chem.*, 2008, **73**, 2641–2648; (*e*) L. Saya, I. Fernández, F. López and J. L. Mascareñas, *Org. Lett.*, 2014, **16**, 5008–5011.

9 (*a*) E. S. Johnson, G. J. Balaich and I. P. Rothwell, *J. Am. Chem. Soc.*, 1997, **119**, 7685–7693; (*b*) J. A. Varela, S. G. Rubín, C. González-Rodríguez, L. Castedo and C. Saá, *J. Am. Chem. Soc.*, 2006, **128**, 9262–9263; (*c*) M. Gulías, A. Collado, B. Trillo, F. López, E. Oñate, M. A. Esteruelas and J. L. Mascareñas, *J. Am. Chem. Soc.*, 2011, **133**, 7660–7663.

10 (*a*) M. Hatano and K. Mikami, *J. Am. Chem. Soc.*, 2003, **125**, 4704–4705; (*b*) L. Bai, Y. Yuan, J. Liu, J. Wu, L. Han, H. Wang, Y. Wang and X. Luan, *Angew. Chem., Int. Ed.*, 2016, **55**, 6946–6950; (*c*) T. Shu, L. Zhao, S. Li, X.-Y. Chen, C. von Essen, K. Rissanen and D. Enders, *Angew. Chem., Int. Ed.*, 2018, **57**, 10985–10988; (*d*) Z. Ding, Y. Wang, W. Liu, Y. Chen and W. Kong, *J. Am. Chem. Soc.*, 2021, **143**, 53–59.

11 K.-H. Rui, S. Yang, Y. Wei and M. Shi, *Org. Chem. Front.*, 2019, **6**, 2506–2513.

12 (*a*) L. Xu, Q. Zhu, G. Huang, B. Cheng and Y. Xia, *J. Org. Chem.*, 2012, **77**, 3017–3024; (*b*) Y. Park, J. Heo, M.-H. Baik and S. Chang, *J. Am. Chem. Soc.*, 2016, **138**, 14020–14029; (*c*) Y.-F. Yang, K. N. Houk and Y.-D. Wu, *J. Am. Chem. Soc.*, 2016, **138**, 6861–6868; (*d*) S. Liu, X. Qi, L.-B. Qu, R. Bai and Y. Lan, *Catal. Sci. Technol.*, 2018, **8**, 1645–1651; (*e*) S. Vásquez-Céspedes, X. Wang and F. Glorius, *ACS Catal.*, 2018, **8**, 242–257; (*f*) Y. Li, H. Chen, L.-B. Qu, K. N. Houk and Y. Lan, *ACS Catal.*, 2019, **9**, 7154–7165; (*g*) H. Xu, M. Bian, Z. Zhou, H. Gao and W. Yi, *ACS Omega*, 2021, **6**, 17642–17650.

13 (*a*) C.-Q. Wang, Y. Zhang and C. Feng, *Angew. Chem., Int. Ed.*, 2017, **56**, 14918–14922; (*b*) H. Xu, W. Chen, M. Bian, H. Xu, H. Gao, T. Wang, Z. Zhou and W. Yi, *ACS Catal.*, 2021, **11**, 14694–14701.

14 B. Wang, Y. Wang, Z. Wang and J. Wang, *Org. Chem. Front.*, 2019, **6**, 2329–2333.

15 (*a*) D. Cassú, T. Parella, M. Solà, A. Pla-Quintana and A. Roglans, *Chem.–Eur. J.*, 2017, **23**, 14889–14899; (*b*) Y. Kawaguchi, A. Nagata, K. Kurokawa, H. Yokosawa and C. Mukai, *Chem.–Eur. J.*, 2018, **24**, 6538–6542.